運輸省港湾技術研究所

港湾技術研究所報告

REPORT OF THE PORT AND HARBOUR RESEARCH INSTITUTE

MINISTRY OF TRANSPORT

VOL. 28 NO. 4 DEC. 1989

NAGASE, YOKOSUKA, JAPAN

港湾技術研究所報告 (REPORT OF P. H. R. I.)

第28巻 第4号 (Vol. 28, No. 4) 1989年12月 (Dec. 1989)

目　　次 (CONTENTS)

REPORT OF THE PORT AND
HARBOUR RESEARCH INSTITUTE
Vol. 28, No. 4 (Dec. 1989)

1. Reproducibility of Directional Random Waves in Laboratory Wave Simulation

Tomotsuka TAKAYAMA*
Tetsuya HIRAISHI**

Synopsis

Cross-spectra of multi-directional waves generated by a serpent-type wave generator have theoretically been derived for both cases of the single and double summation models, which are common synthesis to compute input signals to individual segmented wave-makers. A large number of components are required for the double summation model to eliminate the effects of the phase locking which appears in the theoretically derived cross-spectrum.

Because of an excessively large number of component waves required for the double summation model, the single summation model is recommended to use for laboratory generation of directional waves. Reproducibility of a target directional sprectrum is confirmed by the comaprison with the spectral characteristics of the directional waves generated by the single summation model.

Key Words: Serpent-type Wave Generator, Directional Spectrum, Single Summation Model, Double Snmmation Model, Hydraulic Model Test

* Chief of Wave Laboratory, Hydraulic Engineering Division
** Senior Research Engineer, Hydraulic Engineering Division

港湾技術研究所報告
第28巻 第4号 (1989.12)

1. 実験水槽内における多方向不規則波の再現性の検討

高山 知司*・平石 哲也**

要 旨

実際の海の波に近い多方向不規則波を実験室内に再現することは，模型実験の精度を向上させるためには大変重要なことである。多方向不規則波を造波する装置としてはサーペント型の造波装置が用らいれており，港湾技術研究所においてもこのような造波装置を既に2基製作してきている。

このような造波装置を用いて，目標とする多方向不規則波を造波するためには，個々の造波機へ入力する造波信号を適切にシミュレートする必要がある。現在，造波信号のシミュレーション法としてはシングルサンメーション法とダブルサンメーション法の2種類の方法が一般に採用されている。シングルサンメーション法では各成分波がそれぞれ異なる周波数と波向をもつが，ダブルサンメーション法では，波向は異なるが，ある数の成分波は同じ周波数をもつ。

このような2種類の方法は，成分波の数を非常に多く用いる限りでは，基本的に同じものになることを既に示しているが，実際に造波信号を作成するに当っては造波信号発生装置の記憶容量や演算時間等の制約によってなるべく少ない数の成分波で目標とする多方向波を造波する必要がある。

本論文においては，シングルサンメーション法とダブルサンメーション法とを比較し，どちらが少ない成分波ですむか検討した。そして，造波に必要な成分波数を設定するとともに，実際に造波して，多方向不規則波の方向分布特性を調べた。その結果，以下のような結論を得た。

1) シングルサンメーション法がダブルサンメーション法より少ない成分波数でよいことがわかった。
2) シングルサンメーション法におけるクロススペクトルの値は，波向を設定するときに用いる乱数のシードの値によって変化する。シードを変えてクロススペクトルの値のばらつきを調べた結果では，シングルサンメーション法では少なくとも450の成分波を用いる必要があることがわかった。
3) シングルサンメーション法によって造波した波の方向スペクトル特性を調べた結果，目標に近い波が造波できることがわかった。

キーワード：サーペント型造波装置，方向スペクトル，シングルサンメーション法，ダブルサンメーション法，模型実験

* 水工部 波浪研究室長
** 水工部 主任研究官（浮体運動解析担当）

CONTENTS

1. Introduction

The reproduction of directional random waves similar to real seas is of great importance to perform hydraulic model tests with good accuracy. A serpent-type wave generator, which was originally developed for the generation of regular trains of oblique waves, can be utilized for the generation of short crested waves in a experimental basin. Major hydraulic laboratories in the world have built their serpent-type wave generators and are utilizing them in various model tests (Miles et al. (1986)). The Port and Harbour Research Institute has completed two sets of the serpent-type wave generators of transportable piston type: one consists of 35 segmented wave-makers each with the paddle of 0.8m wide (Takayama et al. (1987)) and the other consists of 30 wave-makers each with the paddle of 0.5m wide.

Two different simulation models of single and double summations are currently employed for the generation of the input signals for multi-directional waves. Few papers (Burcharth et al. (1986), Briggs et al. (1987)) have touched upon the characteristics of directional spreading of laboratory-generated short crested waves. Some other papers (Miles et al. (1987), Jeffery (1987)) have pointed out that the directional random waves simulated by the double summation model do not satisfy the ergodicity of a real sea state because of the phase locking between component waves.

We have examined the characteristics of directional spreading by analizing the theoretical cross spectra of the directional waves generated by the segmented wave-makers for both of the single and double summation models. The analysis concludes that the influence of the phase locking in the double summation model can be eliminated if a large number of frequency components are employed for the simulation. The analysis also shows that both cross-spectra derived from the single and double summation models converge to a same formula as the number of frequency components becomes sufficiently large.

The present paper makes comparison of the single and double summation models in order to verify which model is more appropriate for input signal generation. It also discusses the minimum number of the component waves required for the more appropriate model selected and experimentally confirms the reproducibility of a target waves in a basin.

2. Theoretical Formulation of Cross-Spectrum of Generated Multi-Directional Waves

2.1 Motions of segmented wave paddles

We assume that a wave generator consists of the total number $(N^+ + N^- + 1)$ of segmented wave paddles each with the width b, as shown in **Fig. 1**, where N^+ and N^- represent the numbers of wave paddles placed, respectively, on the positive and negative x-axis whose origin is at the center of a paddle. When each paddle is moved with a constant amplitude and period and with a constant phase lag to the motion of the adjacent paddle, a uniform train of oblique regular waves can be generated in the propagation direction corresponding to the phase lag.

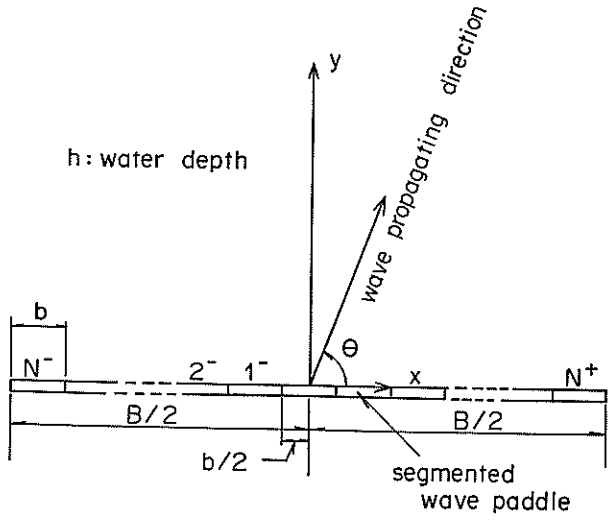

Fig. 1 Coordinates system

Directional random waves can be expressed as a linear superposition of a large number of component waves with different frequencies and propagation directions. Therefore, a simultaneous generation of a number of different oblique waves enables to reproduce directional random waves in a basin. The motions of segmented individual wave paddles are commanded by the input signals, which are prepared by either the single or the double summation model for representation of directional wave profiles. These two representations yield the different formula of the paddle motions as follows:

(1) Single summation model

In this model, a single direction is assigned to each frequency of component waves. Thus, every component wave has different frequency and direction. The movement $\eta_i(t)$ of the i-th segmented wave paddle can be formulated as

$$\eta_1(t)=\sum_{n=1}^{N_s}\frac{a_n}{F_n}\sin(2\pi f_n t-ik_n b\cos\theta_n+\varepsilon_n)\sin\theta_n \qquad (1)$$

where the subscript n indicates the values of the n-th component wave, N_s denotes the total number of component waves in the single summation model, and t, f_n, k_n and θ_n denote the time, the wave frequency, the wave number and the random phase lag of the n-th component wave, respectively. The multiplication by $\sin\theta_n$ in Eq. (1) is made for the purpose of reducing the paddle motion because the oblique wave becomes larger than the wave generated normally.

The wave number k_n ($=2\pi/L_n$: L_n represents the wave length of the n-th component wave) is obtaind as the real value which satisfies the following dispersion relation:

$$(2\pi f_n)^2=k_n g\tanh k_n h \qquad (2)$$

where h and g denote the uniform water depth and the acceleration of gravity.

The amplitude a_n of the n-th component wave is given by

$$a_n=\sqrt{2S(f_n)\,\delta f_n} \qquad (3)$$

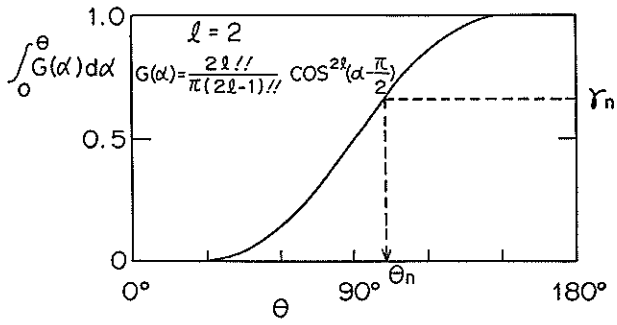

Fig. 2 Selection of wave propagating angle in the single summation model

where $S(f_n)$ and δf_n represent the frequency spectrum and the band width. The representative frequency f_n of the n-th component wave is determined as the central frequency culculated by the second moment of the frequency spectrum within the frequency band width δf_n.

The following Bretschneider-Mitsuyasu spectrum is employed as the frequency spectrum.

$$S(f)=0.257H_{1/3}^2T_{1/3}(T_{1/3}f)^{-5}\exp[-1.03(T_{1/3}f)^{-4}] \qquad (4)$$

Where $T_{1/3}$ and $H_{1/3}$ represent the signification wave period and height of the target random waves, respectively. In this case, the representative frequency f_n of the n-th component can be calculated apporoximately in the following formula:

$$f_n=(1.007/T_{1/3})[\ln(2N_s/(2N-1))]^{-1/4} \quad (n=1,2,\cdots\cdots N_s) \qquad (5)$$

In the single summation model, the representative propagation angle θ_n of the n-th component wave is selected as the angle corresponding to the random value through the cumulative curve $\int_0^\theta G(\alpha;\ f)\ d\alpha$ of the normalized angular spreading $G(\theta;\ f)$.

Figure 2 shows the above selection method of the propagation angle θ_n for a simplified case that the angular spreading is independent from the frequencies of the component waves. In **Fig. 2** γ_n is a value in random value series defined from 0 to 1.

The symbol F_n denotes the transfer function for wave generation and is expressed for a piston type generator by

$$F_n=\frac{2\sinh^2 k_n h}{k_n h\,[1+\sinh\,2k_n h]} \qquad (6)$$

(2) Doudle summation model

In this model, multiple directions are assigned to each frequency of component waves. The movement $\eta_i(t)$ of the i-th segmented paddle is expressed as

$$\eta_i(t)=\sum_{n=1}^{N_D}\sum_{m=1}^{M_D}\frac{a_{nm}}{F_n}\sin(2\pi f_n t-ik_n b\cos\theta_m+\varepsilon_{nm})\sin\theta_m \qquad (7)$$

where the subscripts n and m indicate the values of the n-th frequency and m-th direction, respectively, and N_D and M_D represent the number of component waves in frequency and direction, respectivery. In Eq. (7) ε_{nm} represents the random phase lag defined from 0 to 2π. The multiplication by $\sin\theta_m$ is introduced for the purpose same as described in the single summation model. The wave amplitude a_{nm} is given by

$$a_{nm}=\sqrt{2S(f_n,\ \theta_m)\ \delta f_n\ \delta\theta_m} \tag{8}$$

where $S(f_n, \theta_m)$ represents the directional spectrum at the frequency f_n and the direction θ_m, which is generally expressed as the following product of the frequency spectrum and the angular spreading function:

$$S(f_n,\ \theta_m)=S(f_n)\ G(\theta_m;\ f_n) \tag{9}$$

The representative frequency f_n is given in the same manner as that in the single summation model, and the representative angle θ_m is generally distributed uniformly between 0 to π with a constant interval. In Eq. (8) δf_n and $\delta\theta_m$ are the band width of frequency and propagation angle.

2. 2 Theoretical representation of cross-spectra

When individual paddles of the wave generator are moved as described in the previous section 2. 1, the cross-spectrum of generated random waves can be derived theoretically by applying the formula of oblique waves generated by the segmented paddle motions (Takayama (1982), Takayama and Hiraishi (1987)). The cross-spectrum $\Phi_o\ (f;\ X,\ Y)$ between different two points can be expressed as follows:

$$\Phi_o(f, X, Y)=C_o(f; X, Y)-iQ_o(f; X, Y) \tag{10}$$

where the real and imaginary parts of the cross-spectrum are generally called the co-spectrum $C_o\ (f;\ X,\ Y)$ and quadrature-spectrum $Q_o\ (f;\ X,\ Y)$, respectively, and X and Y represent the spatial lags for x- and y-axes between the two points. The co- and quadrature-spectrua are theoretically given for the single and double summation models as follows:

(1) Single summation model

$$C_o(f_n; X, Y)=\frac{1}{8}S(f_n)\sum_{i=N^-}^{N^+}\sum_{j=N^-}^{N^+}(N^*_{nij}\cos[(i-j)\ k_nb\cos\theta_n]+J^*_{nij}\sin[(i-j)\ k_nb\cos\theta_n])\sin^2\theta_n \tag{11}$$

$$Q_o(f_n; X, Y)=\frac{1}{8}S(f_n)\sum_{i=N^-}^{N^+}\sum_{j=N^-}^{N^+}(N^*_{nij}\sin[(i-j)\ k_nb\cos\theta_n]+J^*_{nij}\cos[(i-j)\ k_nb\cos\theta_n])\sin^2\theta_n \tag{12}$$

where

$$N^*_{nij}=N^*_{in}(x,\ y)\ N^*_{jn}(x+X,\ y+Y)+J^*_{in}(x,\ y)\ J^*_{jn}(x+X,\ y+Y) \tag{13}$$

$$J^*_{nij}=J^*_{in}(x,\ y)\ N^*_{jn}(x+X,\ y+Y)-N^*_{in}(x,\ y)\ J^*_{jn}(x+X,\ y+Y) \tag{14}$$

$$N^*_{in}(x, y)=\int_{ik_nb-k_nb/2}^{ik_nb+k_nb/2}N_o(\sqrt{(k_nx-q)^2+(k_ny)^2})dq \tag{15}$$

$$J^*_{1n}(x,\ y)=\int_{ik_nb-k_nb/2}^{ik_nb+k_nb/2} J_0(\sqrt{(k_nx-q)^2+(k_ny)^2})dq \tag{16}$$

The functions $N_0(x)$ and $J_0(x)$ in Eqs. (15) and (16) represent the Neumann and Bessel functions of the 0-th order, respectively.

The co- and quadrature-spectra expressed by Eqs. (11) and (12) are equal to those of uni-directional regular waves generated by the segmented wave-makers, because a wave frequency has only one wave propagation direction given discretely in a single summation model. Consequently, the directional spreading estimated from the cross-spectra shows the rather sharp and narrow distribution around θ_n. In order to obtain the angular spreading of generated directional waves, a smoothing of the co- and quadrature-spectra must be done in the vicinity of a representative frequency f_n.

If we make smoothing with the number I_r of frequencies in the vicinity of the representative frequency f_n, the smoothed cross-spectrum represented by $C_o(f_n;\ X,\ Y)$ and $Q_o(f_n;\ X,\ Y)$, respectively, at f_n is obtained as

$$C_o(f_n;\ X,\ Y)=\frac{1}{I_r}\sum_{i=1}^{I_r} C_o(f_i;\ X,\ Y) \tag{17}$$

$$Q_o(f_n;\ X,\ Y)=\frac{1}{I_r}\sum_{i=1}^{I_r} Q_o(f_i;\ X,\ Y) \tag{18}$$

As the value of I_r for the smoothing becomes large, the propagation angle θ_n of the n-th component is distributed according to the angular spreading function $G(\theta;\ f)$ and the smoothed co- and quadrature-spectra converge to

$$C_o^*(f_n;\ X,\ Y)=\frac{1}{8}S(f_n)\sum_{m=1}^{M}\sum_{i=-N^-}^{N^+}\sum_{j=-N^-}^{N^+}\{N^*_{nij}\cos[(i-j)k_nb\cos\theta_m]+J^*_{nij}\sin[(i-j)\ k_nb\cos\theta_m]\}\sin^2\theta_m\ G(\theta_m;\ f_n)\delta\theta_m \tag{19}$$

$$Q_o^*(f_n;\ X,\ Y)=\frac{1}{8}S(f_n)\sum_{m=1}^{M}\sum_{i=-N^-}^{N^+}\sum_{j=-N^-}^{N^+}\{N^*_{nij}\sin[(i-j)k_nb\cos\theta_m]-J^*_{nij}\cos[(i-j)\ k_nb\cos\theta_m]\}\sin^2\theta_m\ G(\theta_m;\ f_n)\delta\theta_m \tag{20}$$

where $\delta\theta_m$ represents the angular band width between the adjacent components. Since the spectra expressed by Eqs. (19) and (20) are the ideally obtained ones, they are hereafter called "ideal co- and quadrature-spectra"

(2) Double summation model

When the segmented individual paddle moves as expressed by Eq. (6), the co- and quadrature-spectra can be obtained as follows;

$$C_o(f_n;\ X,\ Y)=\frac{1}{8}S(f_n)\sum_{m=1}^{M_D}\sum_{r=1}^{M_D}\sum_{i=-N^-}^{N^+}\sum_{j=-N^-}^{N^+}\{N^*_{nij}\cos[(i\cos\theta_m-j\cos\theta_r)\ k_nb-(\varepsilon_{nm}-\varepsilon_{nr})]+J^*_{nij}\sin[(i\cos\theta_m-j\cos\theta_r)\ k_nb-(\varepsilon_{nm}-\varepsilon_{nr})]\}\times\sin\theta_m\sin\theta_r\sqrt{G(\theta_m;\ f_n)\ \delta\theta_m}\ \sqrt{G(\theta_r;\ f_n)\ \delta\theta_r} \tag{21}$$

$$Q_o(f_n;\ X,\ Y)=\frac{1}{8}S(f_n)\sum_{m=1}^{M_D}\sum_{r=1}^{M_D}\sum_{i=-N^-}^{N^+}\sum_{j=-N^-}^{N^+}\{N^*_{nij}\sin[(i\cos\theta_m-j\cos\theta_r)\ k_nb-(\varepsilon_{nm}-\varepsilon_{nr})]-J^*_{nij}\cos[(i\cos\theta_m-j\cos\theta_r)\ k_nb-(\varepsilon_{nm}-\varepsilon_{nr})]\}\times\sin\theta_m\sin\theta_r\sqrt{G(\theta_m,\ f_n)\ \delta\theta_m}\ \sqrt{G(\theta_r;\ f_n)\ \delta\theta_r} \tag{22}$$

The above equations indicate that the phase difference of $(\varepsilon_{nm}-\varepsilon_{nr})$ between the two components with same frequency but different directions does not vanish in the representation of the double summation model. The phase difference which remains in Eqs. (21) and (22) is called phase locking. The values of the co- and quadrature-spectra fluctuate greatly, depending on the phase lag given as a uniform random value. The averaging must be done around the representative frequency in order to eliminate the influence of the phase locking.

The mean values of co- and quadrature spectra in the vicinity of f_n also converge to $C_o^*(f)$ in Eq. (19) and Q_o^* (f) in Eq. (20), respectively, as the number for the smoothing I_r become larger.

3. Numerical Determination of Required Number of Component Waves for Generation of Multi-Directional Waves

3.1 Comparison of required number of components between single and double summation models

(1) Simulation condition

We employ the Bretschuneider-Mituyasu type spectrum as the energy frequency spectrum expressed by Eq. (4). **Figure** 3 shows the form of the Bretschneider-Mituyasu type energy spectrum. In **Fig.** 3, f_p represents the peak frequency of the frequency spectrum and f^* represents the non-dimensional frequency (f/f_p). The energy between f_1^* $(=f/f_p=0.80)$ and f_2^* $(=f/f_p=1.37)$ occupies 65% of the total wave energy when f_1^* and f_2^* are selected as the lower and higher frequency at the

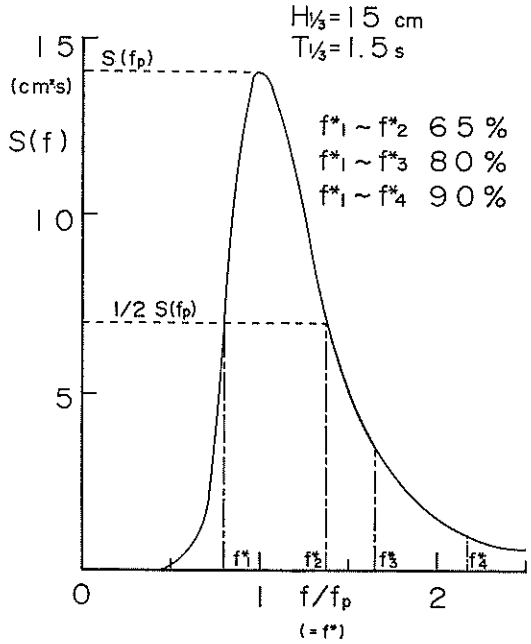

Fig. 3 Bretschneider-Mitsuyasu type spectrum

half value of the spectral peak as shown in **Fig. 3.** Meanwhile 80% of the total energy is occupied in the rangs from f_1^* to f_3^* $(=f/f_p=1.65)$. Therefore good agreement of simulated angular spreading with a target in the effective frequency of f_1^* to f_2^* or f_3^* can be regarded as the confirmation of the validity of laboratory simulation.

We should employ an appropriate form as the angular spreading function $G(\theta;f)$ for the generation of multi-directional waves. Mitsuyasu et al. (1975) has presented the following spreading function derived from various field obsevations:

$$G(\theta;f)=G_0\cos^{2S}\left(\frac{\theta}{2}-\frac{\pi}{4}\right) \quad (0\leq\theta\leq\pi) \tag{23}$$

where G_0 is the constant which satisfies the following normalization:

$$1/\int_0^{\pi} G(\theta;f)\ d\theta=1 \tag{24}$$

and parameter S is related as the frequency as follows;

$$S=\begin{cases} S_{max}(f/f_p)^{-5} & : f<f_p \\ S_{max}(f/f_p)^{-2.5} & : f\geq f_p \end{cases} \tag{25}$$

where S_{max} represents the peak value of S, which has been introduced for the purpose of engineering application (Goda et al. (1975)).

The form of angular spreading function of the Mitsuyasu-type varies largly according with different values of the representative frequency. In order to eliminate the complexity of the spreading function, we employed the following simplified form as an angular spreading function for the simulation condition:

$$G(\theta)=\{(2l)!!/(2l-1)!!\}\cos^{2l}\left(\theta-\frac{\pi}{2}\right) \quad (0\leq\theta\leq\pi) \tag{26}$$

where $(2l)!!=2l\cdot(2l-2)\cdots\cdots4\cdot2$ and $(2l-1)!!=(2l-1)\cdot(2l-3)\cdots\cdots3\cdot1$.

Figures 4 (a), (b), (c) show comparisons of the angular spreading function of the Mitsuyasu type for $S_{max}=75$, 25 and 10 with the simplified form, respectively. In these figures $\tilde{\theta}$ represents the angle deviated from the predominant direction as $\tilde{\theta}=\theta-\pi/2$. Since these angular spreadings of Mitsuyasu type and simplified form are quite symmetric to the predominant direction of $\tilde{\theta}=0^0$, the angular distribution of the Mitsuyasu type is drawn in the region of $\tilde{\theta}>0^0$ and that of the simplified form is drawn in the region of $\tilde{\theta}<0^0$ in these figures. As shown in **Fig.** 4 (a), the angular distribution of the Mitsuyasu-type for $S_{max}=75$ in the effective frequency range $(f^*_1\sim f^*_3)$ of the Bretschneider Mitsuyasu frequency spectrum corresponds to the simplified form with the parameter l more than 5. In case of $S_{max}=25$ shown in **Fig.** 4 (b), the angular spreadings of the Mitsuyasu type at the frequency of f_1^* and f_3^* are very close each other and can be approximated by the distribution of the simplified form with l of about 2. The highest concentration distribution at f^*_0 can be approximated by the simplified form with $l=5$. Thus the angular spreading of the Mitsuyasu type for $S_{max}=25$ in the effective frequency range corresponds to the simplified form with the parameter l between about 2 and 5. In case of $S_{max}=10$ shown in **Fig.** 4 (c), the distribution of the Mitsuyasu-type angular spreading in the effective range between f^*_1 and f^*_3 is approximated by the simplified form with $l=1$ to 3. Thus the distribution of the Mitsuyasu-type angular spreading for S_{max} of 10 to 75 is approximated by the distribution with the parameter l more than 1. In the following simulation, we selected the parameter l of 1 to 5 for the simplified distribution.

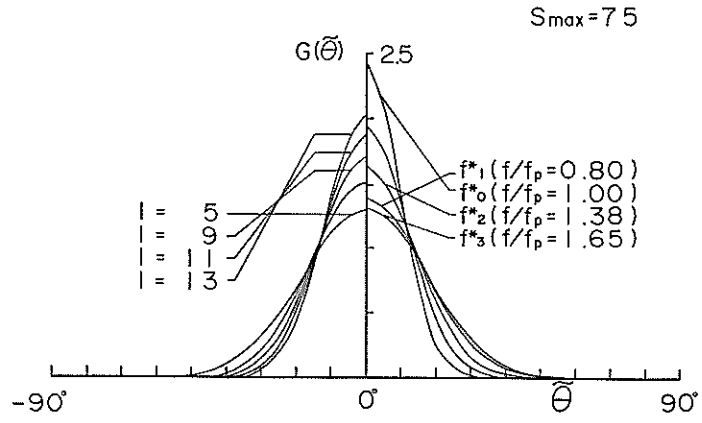

(a) $S_{max}=75$

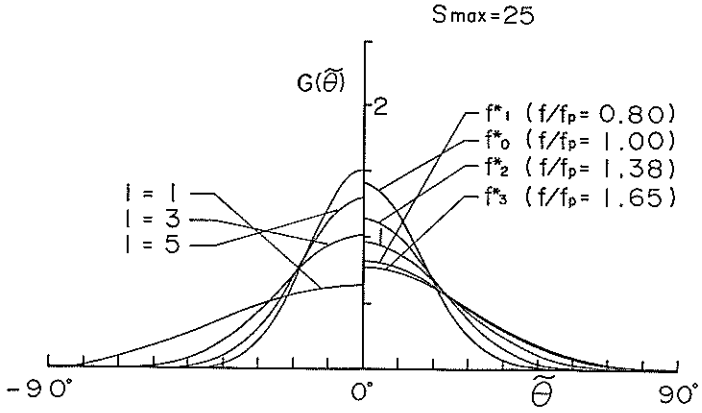

(b) $S_{max}=25$

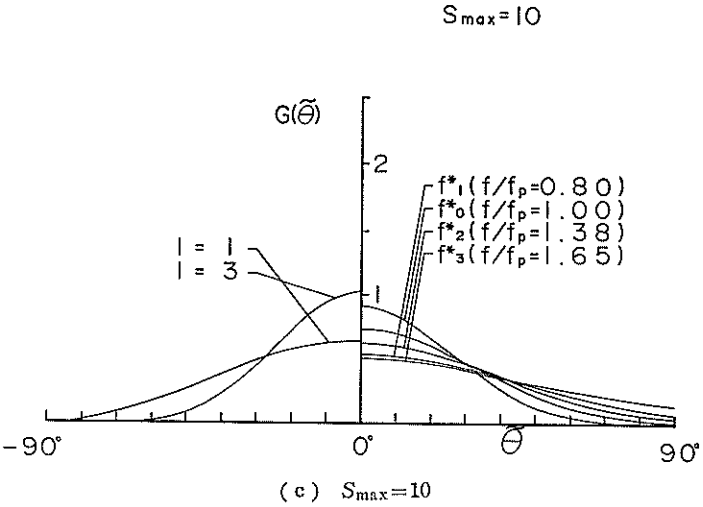

(c) $S_{max}=10$

Fig. 4 Comparison of angular spreadings in Mitsuyasu model and simplified form

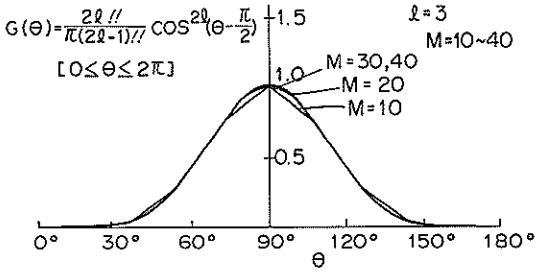

Fig. 5 Approximation of simplified angular spreading function for variation of angular distribution number M

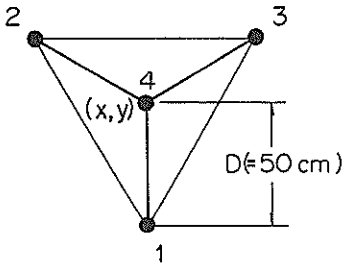

Fig. 6 Array of calculation points

Figure 5 shows the shape of the simplified angular distribution with the parameter $l=3$. In the figure, M indicates the number of directional components. The figure shows that the distribution can be smoothly approximated if we employ the value of M more than 30. Therefore, the number of the directional components is determined to be 30 for the simulation.

Figure 6 shows the array of calculation points for the computation of the cross-spectrum. In **Fig. 6,** D indecates the mimimum distance between each two points. **Table** 1 shows simulation conditions, where L_p denotes the wavelength at the spectral peak frequency and (x, y) represents the position of the centroid of the equilateral triangular shown in **Fig. 6.**

(2) Comparison of the value of cross-spectra in the single and double summation models

As mentioned in the previous section, smoothing of the values of the co- and quadrature-spectrua must be done around the representative frequency of f_n to obtain a smooth angular spreading in both of the single and double summation models. **Figure** 7 shows the example of the variations of the dimensionless co- and quadrature-spectra to the number I_r of components for smoothing. The nondimensioning of these spectra is made by dividing them by the value of the frequency spectrum at the selected frequency. **Figures** 7 (a), (b) and (c) represent the cases for $l=1, 2$ and 5, respectively. The smoothed co- and quadrature spectra are indicated by small circles and squares, respectively, in the figure. The white and black marks correspond to the values computed for the double and single summation models.

In case of $l=1$ shown in **Fig.** 7 (a), the smoothed co- and quadrature-spectra computed for both of the single and double summation models become very close to

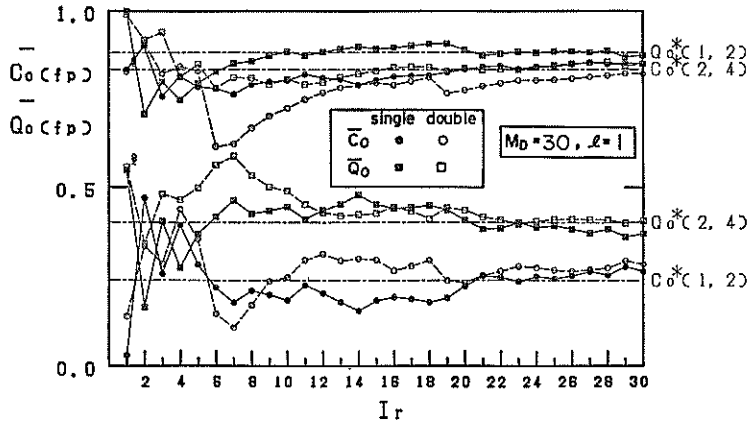

(a) $l=1$

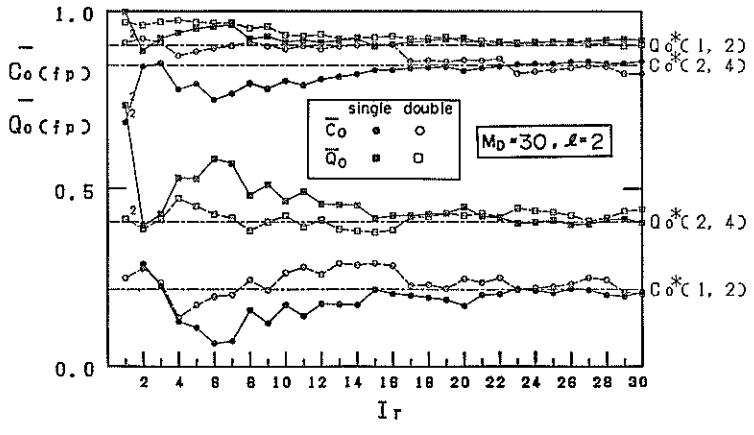

(b) $l=2$

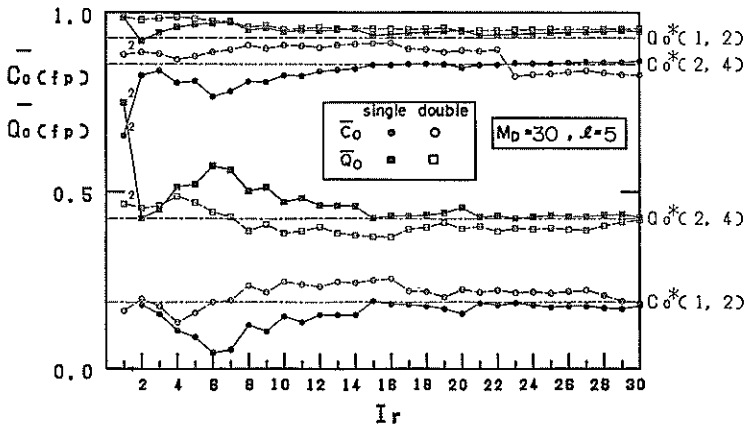

(c) $l=5$

Fig. 7 Variation of dimensionless cross-spectra to the frequency number I_r for smoothing

the corresponding ideal ones represented by C_o^* and Q_o^* when the value of I_r is more than 22. In case of $l=2$ shown in **Fig. 7** (b), the nondimensional values of smoothed co- and quadrature-spectra become very close to the corresponding ideal value for both of the single and double snmmation models with the number of I_r more than 17.

Figure 7 (c) shows that the values of co- and quadrature spectra for $l=5$ converge to the corresponding ideal ones for both of the single and double summation models when the value of I_r is more than 17. However the convergency in the single summation model seems better than that in the double summation model because the values of C_o and Q_o in the single summation model are closer to corresponding ideal ones than those in the double summation model.

Thus, in all cases shown in **Fig. 7,** the smoothed value of cross-spectrum for both of the single and double summation models can converge to the corresponding ideal ones represented by C_o^* and Q_o^* when the number of smoothing, I_r, becomes more than about 20. Consequently we determined the required number for smoothing to be about 20 for both single and double summation models.

For the single summation model, the required total number of component waves become 600 (30x20) if we employ 30 as the number of representative frequency. For the double summation model in contrast to the single summation model, the required total number of component wave calculated as products of I_r, M and N becomes 18000 if the number 30 of the directional components is asigned to each representative frequencies. Thus, the double summation model requires much larger number of the components for the generation of target multi-directional waves than the single summation model. This concludes that the single summation model is superior to the double summation model for the laboratory generation of directional waves. Therefore we make subsequent discussion only on the single summation model.

3.2 Determination of required number of components for the single summation model

The value of the co- and quadrature-spectra in the single summation model varies with a selected value of a seed number in a caluculation algorism of a series of random values which is necessary for the selection of the directional angle of each component wave. A different value of a seed number yields different series of uniform random value. **Figure** 8 shows an example of the variations of the co- and quadrature

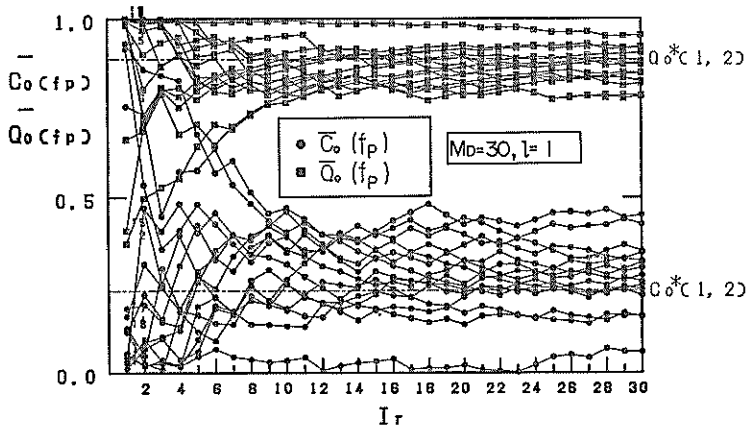

Fig. 8 Variation of dimensionless cross-spectra in the single summation model with different seed numbers

spectra computed for 15 different seed numbers. As shown in **Fig. 8**, most values of co- and quadrature-spectra converge to the corresponding ideal value as I_r becomes more than 15, but few values of the co- and quadrature-spectra do not become close to the corresponding ideal ones even if the value of I_r reaches to 30.

To examine their standard deviation from the ideal ones with a lot of different random seeds, We calculated a hundred values of co- and quadrature-spectra between the two point of 1 and 2 for a hundred different seeds.

Figure 9 show the variations of the standard deviations against the value of I_r.

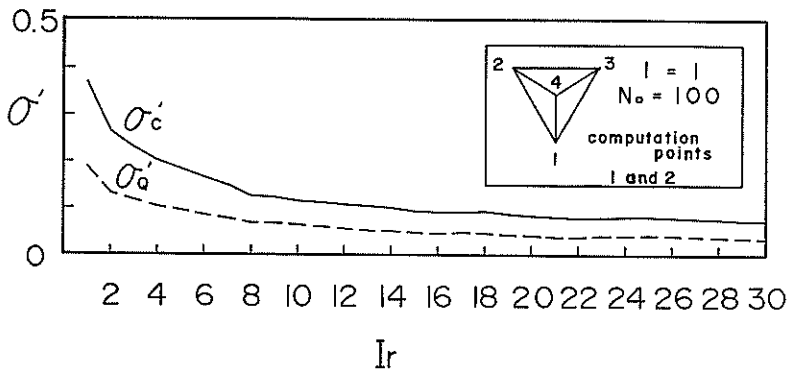

(a) l=1

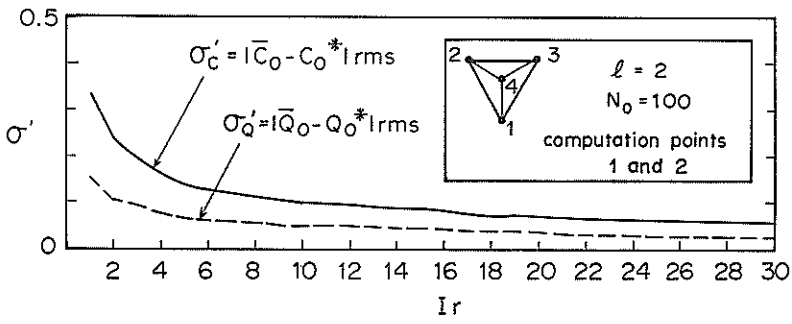

(b) l=2

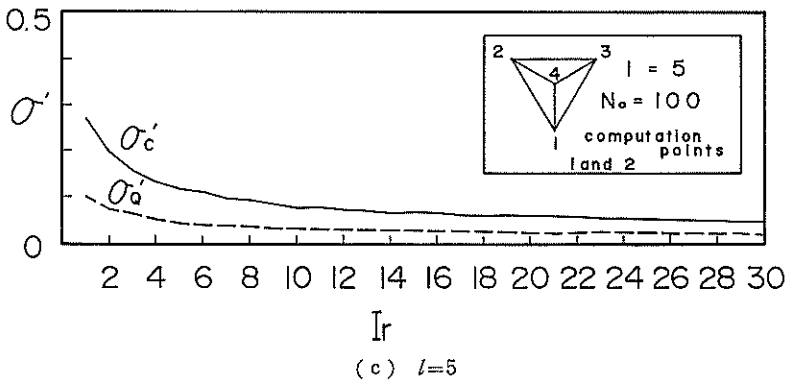

(c) l=5

Fig. 9 Variation of standard deviation of difference between mean and cross-spectra in the single summation model

Figures 9 (a), (b) and (c) show the variation of the deviations in cases of $l=1$, 2 and 5, respectivery.

For those cases, the standard deviations rapidly decrease as I_r increases until 15, but their decreases become gradual as the value of I_r is larger than 15. It is not effective to employ the large number of I_r as many as 20 or 30 under the consideration that larger number of the components consumes more computation time for the simulation. Referring to the variation of the standard deviation to the value of I_r, we determine the minimum required number for smoothing for the single summation model as 15 The total number of components for the generation of multi-directional waves becomes 450 if we employ 30 as the number of representative frequencies. However the number of 450 indicates the minimum number of the components to be employed for the reproduction of directional waves in a laboratory. Furthermore, we must keep it in mind that the directional spectrum of generated waves are slightly different from the target, depending on the selected seed number, even if the value of I_r is selected as 15.

4. Experimental Confirmation of the Reproducibility of Target Directional Waves

4.1 Experimental facilities and conditions

In order to confirm the reproducibility of directional waves simulated by the single summational model, the experiments were carried out in the conditions shown in **Table 1.** **Figure 10** shows the experimental basin and the alocation of experimental equipments like a wave generator and wave gauges installed in a star array. As shown in **Fig. 10,** the basin is surrounded by wave absorbers placed to prevent wave reflection from the side walls.

The Mitsuyasu angular spreading expressed by Eq. (22) was employed as the target. The directional waves with three different target distributions for $S_{max}=25$, 50 and 75 were generated by the serpent-type generator composed of 30 segmented piston-type wave-makers each with a paddle of 50cm wide as shown in **Fig. 10.**

The input signals to the individual wave-makers were simulated by the linear superposition of 1000 components for $S_{max}=25$ and for $S_{max}=75$ and of 500 components for $S_{max}=50$. The generated directional waves were simultaneously observed by a set of four capacitance-type wave gauges placed at the distance 6m away from the paddle line.

Table 1 Computation condition

N	M_D	D	$T_{1/3}$	b	$N^+ + N^- + 1$	B	L_D	(x, y)
		cm	s	cm		cm	cm	cm
30	30	50	1.5	50	30	1500	320	(0, 600)

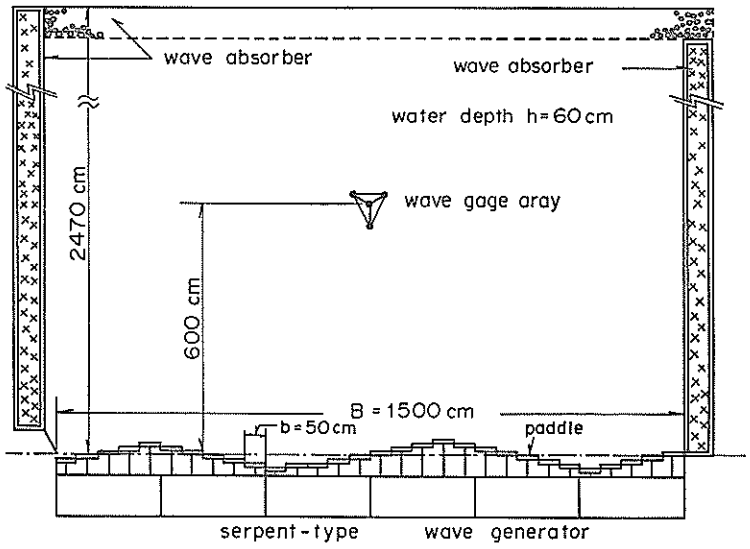

Fig. 10 Overview of the experimental basin

4.2 Comparison of experimental angular spreadings with theoretical and target ones

The experimental cross-spectra among the measurement points are computed by using simultaneously measured wave profiles, and the theoretical cross-spectra are computed as ideal cross-spectra for the angular spreading of the Mitsuyasu-type same as employed in the experiments. The directional characteristics were analysized by the Basian Directional Spectrum Method which has been developed by Hashimoto and Kobune (1988) and seems to be the most reliable estimation method for directional spectrum. In the analysis of directional spreadings in the experiments, the co- and quadrature-spectra were evaluated as the averaged values after smoothing. The number of frequencies for smoothing, which is equivalent to the value of I_r, was employed as 20. The angular spreading derived from the theoretically computed ideal co- and quadrature-spectra may be different from the target one because of the finite width of the individual paddle and the finiteness of the total paddle width of the generator. Therefore the experimental angular spreadings were compared with the theoretically derived ones.

Figures 11 show the comparison between experimental angular spreadings with the theoretically derived spreadings and the targets in the frequency range in which more than 50% of the total energy is occupied. The comparisons for $S_{max}=25$, 75 and 50 are shown in **Figs. 11** (a), (b) and (c), respectivery, where the thick solid and dash lines indicate the angular spreadings experimentally obtained and theoretically caluculated and the thin solid line indicates the target.

In **Fig. 11** (a) for $S_{max}=25$, the peak values of the theoretical angular distributions are higher than those of the targets for $f/f_p=0.92$ and 1.07 and more concentrated around the predominanant direction of 90°. The experimental spreadings are more widely distributed than the theoretically calculated one for the above frequencies. However for higher frequency of $f/f_p=1.53$ these three angular spreadings show quite good agreement each other.

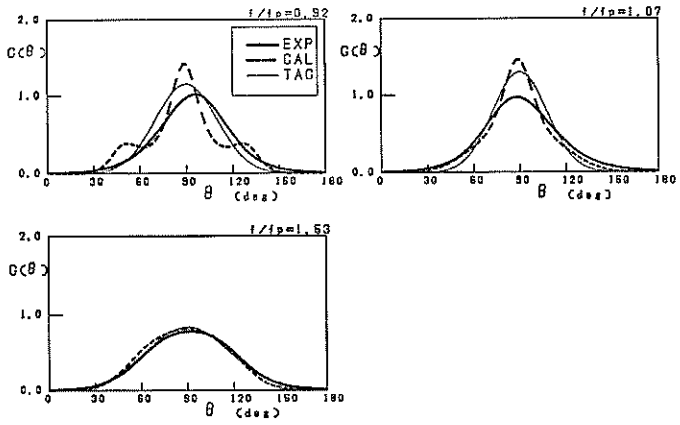

(a) $S_{max}=25$ and $N_s=1000$

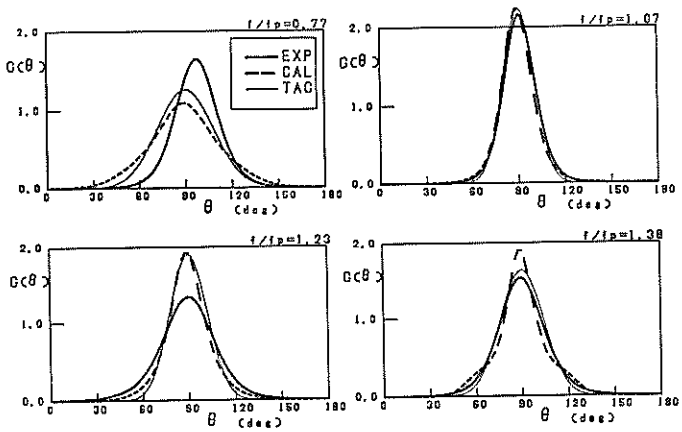

(b) $S_{max}=75$ and $N_s=1000$

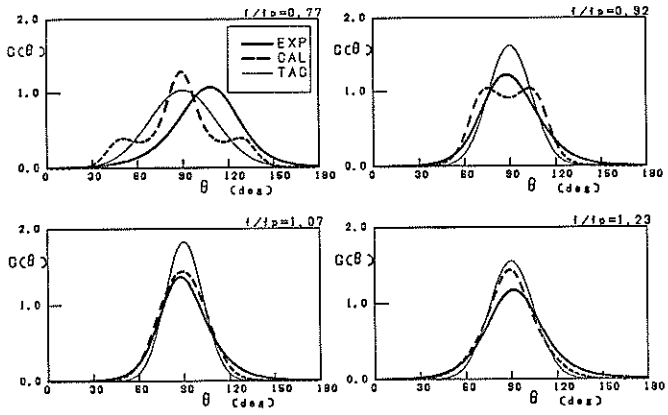

(c) $S_{max}=500$ and $N_s=1000$

Fig. 11 Comparison of angular spreadings between experiment and computation

In **Fig. 11** (b) for $S_{max}=75$, the theoretical spreadings well agree with the corresponding targets in all cases. The experimental spreading also well agrees with the two others for cases of $f/f_p=1.07$ and 1.38, though it is more concentrated for case of $f/f_p=0.77$ and more widely distributed for the case of $f/f_p=1.23$ than the theoretically calculated spreading.

In **Fig. 11** (c) for $S_{max}=50$, the theoretical spreading has two and three peaks for two cases of $f/f_p=0.92$ and 0.77, respectively, though the target is given as one-peakened spreading. This deformation of the theoretical spreading is supposed to be caused by the finiteness of individual or total paddle widths. On the other hand, the experimental spreading is estimated as one peakened distribution for the same cases. The difference between the experimental and theoretically calculated spreadings may be caused by the nonlinearity of real water waves which induces the smoothing of wave directionality. For the cases other than $f/f_p=0.77$, the experimental spreading relatively well agrees the theoretically calculated ones.

5. Conclusions

The following conclusions can be drawn from the present investigation on the generation model for directional random waves.

(1) Since the single summation model assigns a single direction to each frequency of a component wave, the cross-spectrum derived theoretically has a value only at each given frequency and direction and its value fluctuates greatly. To obtain a smooth angular spreading the smoothing of the cross-spectra must be done in the vicinity of the representative frequency.

(2) In the double summation model, which assigns multi-directions to each frequency of the components, the phase locking appears and greatly fluctuates the value of the cross-spectrum. To eliminate the influence of the phase locking the values of the cross-spectra must be smoothed in the vicinity of the representative frequency.

(3) The values of co- and quadrature spectra, which correspond to the real and imaginary part of the cross-spectrum, converge to those of the ideal co- and quadrature-spectra for both of the single and double summation model when the number I_r of frequency for smoothing becomes large.

(4) Judging from the convergence of the cross-spectra to the ideal ones, the required number of the component waves is much smaller in the single summation model than in the double summation model. Thus the single summation model is more appropriate for the reproduction of directional waves in a basin than the double summation model

(5) The smoothed values of co- and quadrature-spectra depend on a selected seed numder in a calculation algorism for the selection of the directional angles. The result of the computation for a hundred different seeds shows that the standard deviations of averaged co- and quadrature-spectra from the corresponding ideal values rapidly decrease as I_r increases until 15, but their decreases become gradual as the value of I_r is larger than 15. It is effective to employ 15 as the required number I_r for smoothing in the single summation model. In order to reproduce the target multi-directional waves in the single summation model the number 450 is required as the minimum number of the components.

(6) The directional random waves were generated in our basin for the various input signals simulated by the single summation model. The comparisons of the wave directionalities in the experiments and computations confirm good reproducibility of the single summation model for the generation of the multi-directional waves in a basin

(*Received on Sept. 30, 1989*)

Acknowledgement

The authors wish to express their sincere gratitude to Dr. Yoshimi Goda, Professor of Civil Engineering Depatment, Yokohama National University, for his useful suggestions and discussions. A special debt of gratitude is owed to Mr. Noriaki Hashimoto, senior research engineer of Marine Hydrodynamics Division, for his lecturing accuracy of the estimate of directional spectrum and his presenting the program of BDM. The authors also express their thanks to Mr. Yoshihiro Tateishi, the member of the Wave Laboratory, for his assistance in performing the experiments and the computations.

The present research work was supported by the fundamental research fund from the Agency of Science and Technology.

References

Briggs M. J., L. E. Borgman and D. G. Outlaw (1987) : Generation and analysis of directional spectral waves in a laboratory basin. *Proc. 19th Offshore Technology Conf.*, pp.495～502.

Burcharth H. F., S. R. K. Nielsen and K. Schaarup-Jensen (1986): A three dimensional sea facility for deep and shallow water waves, *Proc. 5th International Offshore Mechanics and Arctic Eng. Symposium*, pp. 72～79.

Goda Y. and Y. Suzuki (1975),: Computation of refraction and diffraction of sea waves with Mitsuyasu's directional spectrum *Tech. Note of Port and Harbour Res. Inst.*, No. 230, 45p. (inJapanese)

Jefferys E. R. (1987),: Directional seas should be ergodic *Applied Ocean Research*, Vol. 9, No. 4, pp. 186～191.

Hashimoto N. and K. Kobune (1988),: Directional spectrum estimation from a Bayesian approach *Proc. 21st I. C. C. E.*

Miles M. D., P. H. Laurich and E. R. Funke (1986) : A multi mode segmented wave generator for the NRC Hydraulic Laboratory, *Proc. 21st American Tank Conf.*, Washington, D. C.

Miles M. D. anf E. R. Funke (1987) : A comparison of methods for synthesis of directional seas, *Proc. 6th International Offshore Mechanics and Arctic Eng.* Symposium, pp. 247～255.

Mitsuyasu, H. et al, (1975) : Obsevation of the directional spectrum of ocean waves using a cloverleaf bouy, *Jour. Physical Oceanogr.*, Vol. 5, No. 4, pp. 750～760.

Takayama T. (1982) : Theoretical properties of oblique waves generated by serpent-

type wave-makers, *Rept. Port and Harbour Res. Inst.* Vol. 21, No. 2, pp. 3～48.
Takayama T. and T. Hiraishi (1987),: Fundamental characteristics of oblique regular waves and directional random waves general by a serpent-type wave generator *Rept. of Port and Harbour Res. Inst.*, Vol. 26, No, 5, pp. 101～136.

List of main Symbols

a_n : Amplitude of n-th component wave
a_{nm} : Amplitude of nm-th component wave
B : Total paddle width of wave generator
b : Width of individual paddle width
$C_o(f; x, y)$: Co-spectrum
F_n : Transfer function of n-th component wave
f_n : Frequency of n-th component wave
$G(\theta; f)$: Angular spreading function
G_o : Constant for normalization of angular spreading
g : Acceleration of gravity
$H_{1/3}$: Significant wave height
h : Water depth
$J_o(x)$: Bessel function on the 0-th order
k_n : Wave number of n-th component wave
l : Concentration parameter of simprified angular distribution
M : Number of directional components
M_D : Number of directional components in double summation model
N : Number of frequency components
N_S : Number of frequency components in single summation model
N_D : Number of frequency components in double summation model
N^+ : Number of wave paddle on the positive x-axis
N^- : Number of wave paddles on the negative x-axis
$N_o(x)$: Neumann function of the 0-th order
$Q_o(f; x, y)$: Quadrature-spectrum
$S(f)$: Frequency spectrum
$S(f, \theta)$: Directional spectrum
S_{max} : Wave energy concentration parameter
$T_{1/3}$: Significant wave period
t : Time
X : Spetial lag
x : Spetial axis
Y : Spetial lag
y : Spetial axis
γ_n : Random value for determination of wave propagation direction
δf_n : Frequency band width of the n-th component wave
$\delta\theta_m$: Directional band width of the m-th component wave
ε_n : Phase lag of the n-th component wave
ε_{nm} : Phase lag of the nm-th component wave
$\eta_i(t)$: Motion of the i-th paddle
θ_n : Propagation angle of n-th component